Microfluidic Nano-Scale qPCR Enables Ultra-Sensitive and Quantitative Detection of SARS-CoV-2

Authors:

Xin Xie, Tamara Gjorgjieva, Zaynoun Attieh, Mame Massar Dieng, Marc Arnoux, Mostafa Khair, Yasmine Moussa, Fatima Al Jallaf, Nabil Rahiman, Christopher A. Jackson, Lobna El Messery, Khristine Pamplona, Zyrone Victoria, Mohammed Zafar, Raghib Ali, Fabio Piano, Kristin C. Gunsalus, Youssef Idaghdour

Date Submitted: 2021-05-25

Keywords: detection, viral load, viral RNA, ultra-sensitive, nano-qPCR, microfluidics, COVID-19, SARS-CoV-2

Abstract:

A major challenge in controlling the COVID-19 pandemic is the high false-negative rate of the commonly used RT-PCR methods for SARS-CoV-2 detection in clinical samples. Accurate detection is particularly challenging in samples with low viral loads that are below the limit of detection (LoD) of standard one- or two-step RT-PCR methods. In this study, we implemented a three-step approach for SARS-CoV-2 detection and quantification that employs reverse transcription, targeted cDNA preamplification, and nano-scale qPCR based on a commercially available microfluidic chip. Using SARS-CoV-2 synthetic RNA and plasmid controls, we demonstrate that the addition of a preamplification step enhances the LoD of this microfluidic RT-qPCR by 1000-fold, enabling detection below 1 copy/µL. We applied this method to analyze 182 clinical NP swab samples previously diagnosed using a standard RT-qPCR protocol (91 positive, 91 negative) and demonstrate reproducible and quantitative detection of SARS-CoV-2 over five orders of magnitude (<1 to 106 viral copies/µL). Crucially, we detect SARS-CoV-2 with relatively low viral load estimates (<1 to 40 viral copies/µL) in 17 samples with negative clinical diagnosis, indicating a potential false-negative rate of 18.7% by clinical diagnostic procedures. In summary, this three-step nano-scale RT-qPCR method can robustly detect SARS-CoV-2 in samples with relatively low viral loads (<1 viral copy/µL) and has the potential to reduce the false-negative rate of standard RT-PCR-based diagnostic tests for SARS-CoV-2 and other viral infections.

Record Type: Published Article

Submitted To: LAPSE (Living Archive for Process Systems Engineering)

Citation (overall record, always the latest version):	LAPSE:2021.0426
Citation (this specific file, latest version):	LAPSE:2021.0426-1
Citation (this specific file, this version):	LAPSE:2021.0426-1v1

DOI of Published Version: https://doi.org/10.3390/pr8111425

processes

MDPI

Article

Microfluidic Nano-Scale qPCR Enables Ultra-Sensitive and Quantitative Detection of SARS-CoV-2

Xin Xie [1], Tamara Gjorgjieva [2,3], Zaynoun Attieh [1], Mame Massar Dieng [2], Marc Arnoux [4], Mostafa Khair [4], Yasmine Moussa [1], Fatima Al Jallaf [2,3], Nabil Rahiman [1], Christopher A. Jackson [5], Lobna El Messery [6], Khristine Pamplona [6], Zyrone Victoria [6], Mohammed Zafar [6], Raghib Ali [3], Fabio Piano [1,5], Kristin C. Gunsalus [1,3,5,*] and Youssef Idaghdour [2,3,*]

1 Center for Genomics and Systems Biology, New York University Abu Dhabi, P.O. Box 129188, Abu Dhabi 51133, UAE; xx12@nyu.edu (X.X.); za2061@nyu.edu (Z.A.); yasminemoussa@nyu.edu (Y.M.); nabil.rahiman@nyu.edu (N.R.); fp1@nyu.edu (F.P.)
2 Program in Biology, Division of Science, New York University Abu Dhabi, P.O. Box 129188, Abu Dhabi 51133, UAE; tg1407@nyu.edu (T.G.); mmd14@nyu.edu (M.M.D.); fa69@nyu.edu (F.A.J.)
3 Public Health Research Center, New York University Abu Dhabi, P.O. Box 129188, Abu Dhabi 51133, UAE; ra107@nyu.edu
4 Core Technology Platforms, New York University Abu Dhabi, P.O. Box 129188, Abu Dhabi 51133, UAE; mga5@nyu.edu (M.A.); mrk6@nyu.edu (M.K.)
5 Department of Biology and Center for Genomics and Systems Biology, New York University, New York, NY 10003, USA; cj59@nyu.edu
6 Proficiency Healthcare Diagnostics, Electra Street, Abu Dhabi 51133, UAE; dr.l.elmessery@proficiencylab.org (L.E.M.); khristinep@proficiencylab.org (K.P.); zyronev@proficiencylab.org (Z.V.); zafar.m@proficiencylab.org (M.Z.)
* Correspondence: kcg1@nyu.edu (K.C.G.); youssef.idaghdour@nyu.edu (Y.I.)

Received: 30 September 2020; Accepted: 25 October 2020; Published: 9 November 2020

Abstract: A major challenge in controlling the COVID-19 pandemic is the high false-negative rate of the commonly used RT-PCR methods for SARS-CoV-2 detection in clinical samples. Accurate detection is particularly challenging in samples with low viral loads that are below the limit of detection (LoD) of standard one- or two-step RT-PCR methods. In this study, we implemented a three-step approach for SARS-CoV-2 detection and quantification that employs reverse transcription, targeted cDNA preamplification, and nano-scale qPCR based on a commercially available microfluidic chip. Using SARS-CoV-2 synthetic RNA and plasmid controls, we demonstrate that the addition of a preamplification step enhances the LoD of this microfluidic RT-qPCR by 1000-fold, enabling detection below 1 copy/µL. We applied this method to analyze 182 clinical NP swab samples previously diagnosed using a standard RT-qPCR protocol (91 positive, 91 negative) and demonstrate reproducible and quantitative detection of SARS-CoV-2 over five orders of magnitude (<1 to 10^6 viral copies/µL). Crucially, we detect SARS-CoV-2 with relatively low viral load estimates (<1 to 40 viral copies/µL) in 17 samples with negative clinical diagnosis, indicating a potential false-negative rate of 18.7% by clinical diagnostic procedures. In summary, this three-step nano-scale RT-qPCR method can robustly detect SARS-CoV-2 in samples with relatively low viral loads (<1 viral copy/µL) and has the potential to reduce the false-negative rate of standard RT-PCR-based diagnostic tests for SARS-CoV-2 and other viral infections.

Keywords: SARS-CoV-2; COVID-19; microfluidics; nano-qPCR; ultra-sensitive; viral RNA; viral load; detection

1. Introduction

The most widely used method for the detection of SARS-CoV-2 (the infectious agent that causes COVID-19) in nasopharyngeal (NP) swab samples is Reverse Transcription Polymerase Chain Reaction (RT-PCR) [1–3]. Inaccurate test results from RT-PCR have been widely reported, with estimated false-negative rates of 10–30% among different implementations of this method [4–7]. Such high false-negative rates pose a significant challenge to controlling the spread of infection, and are further exacerbated by poor sample quality or low viral loads that are below the detection limit of standard RT-PCR methods [8,9]. This, combined with both the cost and scarcity of reagents [10–12], has hampered global scale-up of RT-PCR testing to levels that would be required to adequately monitor communities for COVID-19.

An additional challenge to controlling the spread of COVID-19 is the role of asymptomatic transmission [13–16]. Different estimates suggest that 40 to 80% of infected individuals are either pre-symptomatic, asymptomatic, or mildly symptomatic [17–20]. Early detection of infection in these individuals is crucial for disease control, which is why many countries and communities have started implementing active screening programs that extend COVID-19 testing to asymptomatic individuals. However, asymptomatic carriers sometimes carry very low viral loads [21] that may not be detected by a standard RT-PCR test [22]. Therefore, the development of more sensitive detection methods that can detect low viral loads is crucial.

Most commercial kits for COVID-19 testing utilize either a one-step RT-PCR approach, which combines the RT and qPCR reactions, or a two-step approach in which RT and qPCR are performed sequentially. A target-specific preamplification step has been successfully incorporated in a number of studies to detect and analyze various types of samples with limited amount of genomic materials, including viruses in human samples [23] or in drinking water [24], circulating tumor DNA in blood [25], and even ancient DNA samples [26]. Therefore, in this study, we implemented a three-step approach involving sequential RT, targeted cDNA preamplification, and qPCR, using a commercially available microfluidics platform. Using this method, we demonstrate reliable ultra-sensitive detection of low SARS-CoV-2 viral loads in both standard positive controls and clinical NP swab samples, including samples previously diagnosed as negative by an accredited diagnostic lab. Overall, this microfluidic RT-PCR assay is a cost-effective strategy with the potential to reduce the false-negative rate of clinical diagnostic tests, and as such, could be a valuable tool in active screening programs aimed at the early detection of SARS-CoV-2.

2. Materials and Methods

We first implemented the three-step SARS-CoV-2 detection method using synthetic SARS-CoV-2 RNA and SARS-CoV-2 plasmids and determined the limit of detection, before validating this method in clinical nasopharyngeal swab samples.

2.1. Ethics Statement

This study was determined as exempt by the NYU Abu Dhabi (NYUAD) Institutional Review Board (HRPP-2020-48) as it involves clinical samples that have already been collected by a diagnostic lab for the primary purpose of SARS-CoV-2 testing, and have been de-identified before being transported to and analyzed at NYUAD.

2.2. Positive Controls

Two types of positive controls were used in this study. The Twist Synthetic SARS-CoV-2 RNA (102024, Twist Biosciences, San Francisco, CA, USA) consists of six non-overlapping ssRNA fragments with a coverage of greater than 99.9% of the viral genome. The SARS-CoV-2 plasmids (10006625, IDT, Leuven, Belgium) contain the complete DNA sequence of the SARS-CoV-2 nucleocapsid gene.

2.3. SARS-CoV-2 Detection (Synthetic RNA and Plasmid)

Two assays (primer/probe sets) were used for SARS-CoV-2 detection, per CDC recommendations: 2019-nCoV_N1 and 2019-nCoV_N2 (2019-nCoV CDC EUA Kit, 10006606, IDT). The human RNase P (RP) assay was used as a control for RNA extraction and RT-qPCR reactions. For both positive controls, 10-fold serial dilutions were prepared, with two replicates at each concentration. Each sample was analyzed using 9 replicates for N1, 9 replicates for N2, and 6 replicates for RP assays.

Manual extraction of synthetic SARS-CoV-2 RNA was performed using the ABIOpureTM Viral DNA/RNA Extraction Kit (M561VT50, Alliance Bio, Bothell, WA, USA) according to the manufacturer's instructions. The isolated synthetic RNA/SARS-CoV-2 plasmids were then used for reverse transcription (RT) and quantitative PCR (qPCR) using the Fluidigm Real-Time PCR for Viral RNA Detection protocol (FLDM-00103, Fluidigm, San Francisco, CA, USA). The RT was prepared by mixing 5 µL of purified RNA and 1.25 µL RT Master Mix (100-6297, Fluidigm, San Francisco, CA, USA), followed by 3 steps of incubation using the Bio-Rad T100 thermal cycler (Bio-Rad, Hercules, CA, USA). Preamplification of cDNA was performed by first pooling the N1, N2, and RP assays and diluting into dilution reagent (100-8730, Fluidigm, San Francisco, CA, USA) to a final concentration of 100.5 and 25.5 nM for the primers and probes, respectively, and then, mixing it with 2.5 µL Preamp Master Mix (100-5744, Fluidigm, San Francisco, CA, USA) and 0.635 µL PCR water (100-5941, Fluidigm, San Francisco, CA, USA). The final preamplification reaction (12.5 µL) consisted of preamplification pre-mix and RT reaction in a 1:1 ratio. Upon completion of 20 preamplification cycles, reactions were diluted 1:5 in Dilution Reagent (100-8730, Fluidigm, San Francisco, CA, USA), resulting in a total volume of 62.5 µL.

The qPCR mix was prepared using 1.8 µL of diluted cDNA or SARS-CoV-2 plasmid positive controls (with or without preamplification) and 2 µL of 2X TaqMan Fast Advanced Master Mix (4444557, Thermo Fisher Scientific, Waltham, MA, USA) and 0.2 µL 20X GE Sample Loading Reagent (Fluidigm PN 100-7610). Next, 3 µL qPCR mix from each sample was loaded into the sample inlet in the 192.24 integrated fluid circuit (IFC, Fluidigm, see Figure S1). For each assay, 3 µL of primer/probe mix (13.5X) was mixed with 1 µL of 4X Assay Loading Reagent (Fluidigm, 102-0135), and 3 µL of each assay mixed was loaded in the assay inlet in the 192.24 IFC chip (Fluidigm, 100-626). The chip was then placed in an IFC controller RX machine to pre-load the samples and the assays, and then, loaded onto the BioMark HD instrument (Fluidigm) for RT-qPCR using 35 cycles. In total, 4608 reactions were performed in each 192.24 IFC chip. The raw amplification data were acquired using the Fluidigm data collection software and analyzed using the Fluidigm Real-Time PCR Analysis software 3.0.2. To calculate the Cq (cycle of quantification) of each sample, a global threshold was automatically calculated and applied to all the samples in the chip. The crossing point at which the amplification curve of each sample crossed the threshold line was determined as the Cq. For comparability with other studies, we note that the Cq is numerically equivalent to the Ct value in our system.

2.4. Clinical Samples and SARS-CoV-2 Clinical Diagnostics

A total of 182 de-identified nasopharyngeal (NP) swab samples (91 positive and 91 negatives for SARS-CoV-2) were obtained from an accredited diagnostic lab. The diagnostic lab used the automated NX-48S Viral RNA Kit (NX-48S, Genolution Inc., Seoul, Korea) for RNA extraction, and the U-TOP^{TM} COVID-19 Detection Kit (SS-9930, Seasun Biomaterials Inc., Daejeon, Korea) for SARS-CoV-2 detection, following accredited protocols in the United Arab Emirates that follow guidelines from the US Center for Disease Control and Prevention (CDC). Briefly, three primers were used, two targeting the viral ORF1ab and the N genes, and one acting as an internal control. A sample was classified as positive if at least one of the viral genes was detected with a Ct value ≤38. The reported LoD of the kit was 10 copies/reaction, translating to 1 copy/µL in the RNA sample.

2.5. Three-Step Analysis of SARS-CoV-2 in Clinical Samples

Automated extraction of viral RNA from the clinical samples was performed using the Chemagic 360 automated nucleic acid extraction system (2024-0020, Perkin Elmer, Waltham, MA, USA) and the Chemagic Viral DNA/RNA 300 Kit H96 (CMG-1033S, Perkin Elmer, Waltham, USA) according to the manufacturer's instructions. For RNA extraction, 300 µL clinical samples were used and eluted in 80 µL elution buffers. Subsequent RT, preamplification, and qPCR were performed as described above. Clinical samples were loaded onto two 96-well plates for RT and preamplification, with each plate containing 10-fold serially diluted SARS-CoV-2 plasmid controls (50–5000 copies/µL in the original experiment; 10–10,000 copies/µL in the replication experiments) used for viral load estimation. Samples were considered valid if the RP gene was reliably detected in at least 4 of the 6 replicates. Samples were classified as positive if at least one of the N assays (N1 or N2) was detected in at least one replicate. Each PCR plate also contained two negative controls: empty transport medium, to control for contamination during RNA extraction (NRX control), and TE (Tris–EDTA) dilution buffer, to control for contamination during pre-amplification and qPCR (NQF control).

2.6. Statistical Analysis

Data analysis was performed with R, associated packages, and GraphPad Prism 8. Data were summarized as mean ± standard deviation. Virus copies were quantified based on a 10-fold dilution series of SARS-CoV-2 plasmids to generate standard curves. The standard curves were used to build log-linear models used to predict viral loads based on Cq values.

3. Results

The objective of this study was to evaluate whether a microfluidic nano-scale RT-qPCR system has the potential to enhance the limit of detection (LoD) of SARS-CoV-2 in clinical samples. To do this, we first used synthetic SARS-CoV-2 RNA (Twist RNA) and SARS-CoV-2 plasmids to develop and evaluate our protocols (Figure 1A), and subsequently applied the method to 182 NP samples that were analyzed in a clinical diagnostic lab using standard RT-PCR protocols (Figure 1B). For all our experiments, we used a 192.24 microfluidic chip, which allowed 192 samples to be independently analyzed against 24 different qPCR probes (24 assays), totaling 4608 nano-scale qPCR reactions per experiment (Figure S1A). Following the standards set by the US Center for Disease Control (CDC), we used two probes targeting different regions of the N gene (N1 and N2) for SARS-CoV-2 detection (Figure S1B), and a probe targeting the human Ribonuclease P (RP) gene as a quality control. To increase the robustness of detection for each assay, we performed nine technical replicates for the N1 and N2 assays, and six replicates for the RP assay.

We first used 10-fold dilution series of the synthetic SARS-CoV-2 RNA (Twist RNA) and SARS-CoV-2 plasmid to determine the LoD for the N1 and N2 assays, with and without a preamplification step (Figure 2). With preamplification, the viral N gene was detectable in Twist RNA at 0.5 copies/µL (N1 assay, 9 out of 18 replicates) and 5 copies/µL (N2 assay, 18 out of 18 replicates), whereas without preamplification, we were only able to detect viral material in a few replicates at 5000 copies/µL (N1 assay, 3 out of 18 replicates; N2 assay, 2 out of 18 replicates). No viral material was detected below 5000 copies/µL (Figure 2A). We observed similar results using the SARS-CoV-2 plasmid (Figure 2B), demonstrating that the preamplification step is essential for high detection sensitivity for SARS-CoV-2 in the range of 1 copy/µL. For this reason, we used a preamplification step in all subsequent experiments.

Since the LoD is dependent on the abundance of input material, we next examined the extent to which RNA extraction affects the quantity of input material. We extracted RNA from the Twist RNA dilution series and eluted it in the same volume as the original samples (Figure S2). With or without extraction, we were able to detect 5 copies/µL using both the N1 and N2 assays, but the Cq values for the extracted samples increased by 1–3 cycles at different dilutions. Most viral nucleic acid

extraction kits recommend using carrier RNA to enhance recovery of viral RNA in samples where the quantity of material is low; however, carrier RNA might compete nonspecifically with the SARS-CoV-2 RNA in reverse transcription reactions. To explore this possibility, we added carrier RNA directly into the Twist RNA serial dilutions and found that Cq values indeed increased by 0.9–2.7 cycles at most concentrations (Figure S2). This suggests that the presence of carrier RNA, and not RNA extraction itself, can adversely affect the detection of viral material, possibly by interfering with the efficiency of reverse transcription.

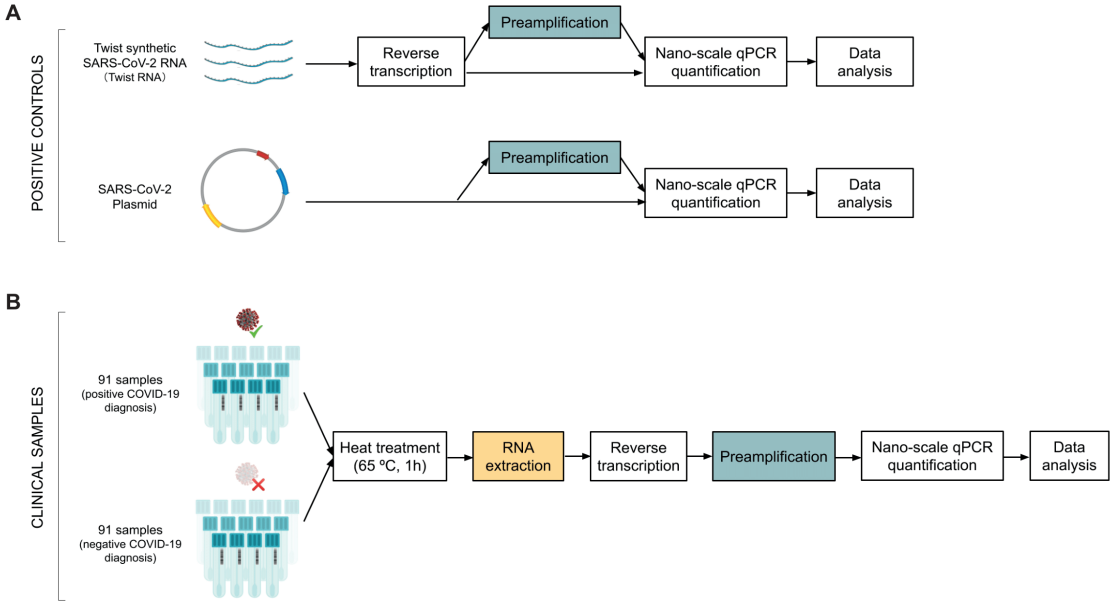

Figure 1. Schematic overview of the experimental design for SARS-CoV-2 RT-qPCR testing using the Fluidigm platform. (**A**) Workflow for method validation in positive controls (SARS-CoV-2 synthetic RNA and SARS-CoV-2 plasmids) with and without a preamplification step. (**B**) Workflow for clinically diagnosed SARS-CoV-2 samples (nasopharyngeal swabs) from an accredited diagnostic lab.

To evaluate the sensitivity of our workflow in comparison with standard SARS-CoV-2 detection methods, we next analyzed 182 NP swab samples previously diagnosed by an accredited diagnostic laboratory as SARS-CoV-2 positive or negative (91 samples each). We heated the samples at 65 °C for 1 h to inactivate viral particles and analyzed them using our SARS-CoV-2 detection workflow (Figure 1B). Any samples with poor qPCR amplification curves and high variation in Cq values among replicates (SEM > 0.5) were flagged as inconsistent, which in our experience is usually due to technical issues such as formation of air bubbles when loading the samples onto the chip. A total of 11 inconsistent samples (4 positive and 7 negative) were removed from subsequent analysis (Figure 3A). The remaining 171 high quality and valid samples were classified as either positive (either N1 or N2 detected) or negative (neither N1 nor N2 detected). Using this classification, we confirmed 86 positive (Pos_Pos, 94.5%) and found 1 negative sample (Pos_Neg, 1.1%) among the 87 samples with a positive clinical diagnosis (Figure 3B). The one Pos_Neg sample had a relatively high Cq value (36.4 for the N-gene and 37.2 for the ORF1 gene) in the clinical diagnostic test; therefore, it is likely that RNA degradation during transport or the heat inactivation process may have brought its viral load below the LoD. Exploring how the two methods compared, we found relative consistency between the ranking of Cq values between the microfluidic RT-qPCR test and the clinical diagnostic test, despite the expected difference in Cq values due to the addition of a pre-amplification step (20 cycles) in the microfluidic method (Figure S3). Among the 84 samples with a negative diagnosis, we detected 17 positives (Neg_Pos, 18.7%): in 9 of these samples, we obtained valid Cq values for all 18 replicates (both N1 and N2), and in the remaining 9, we detected the virus in 9/18 replicates (either all N1 or all N2). All samples with a negative clinical diagnosis showed no detectable signal in the clinical diagnostic qPCR test. These analyses thus show

that by performing a large number of replicates, our method can robustly and consistently detect SARS-CoV-2 and identify samples as false-negatives by the clinical diagnostic procedure.

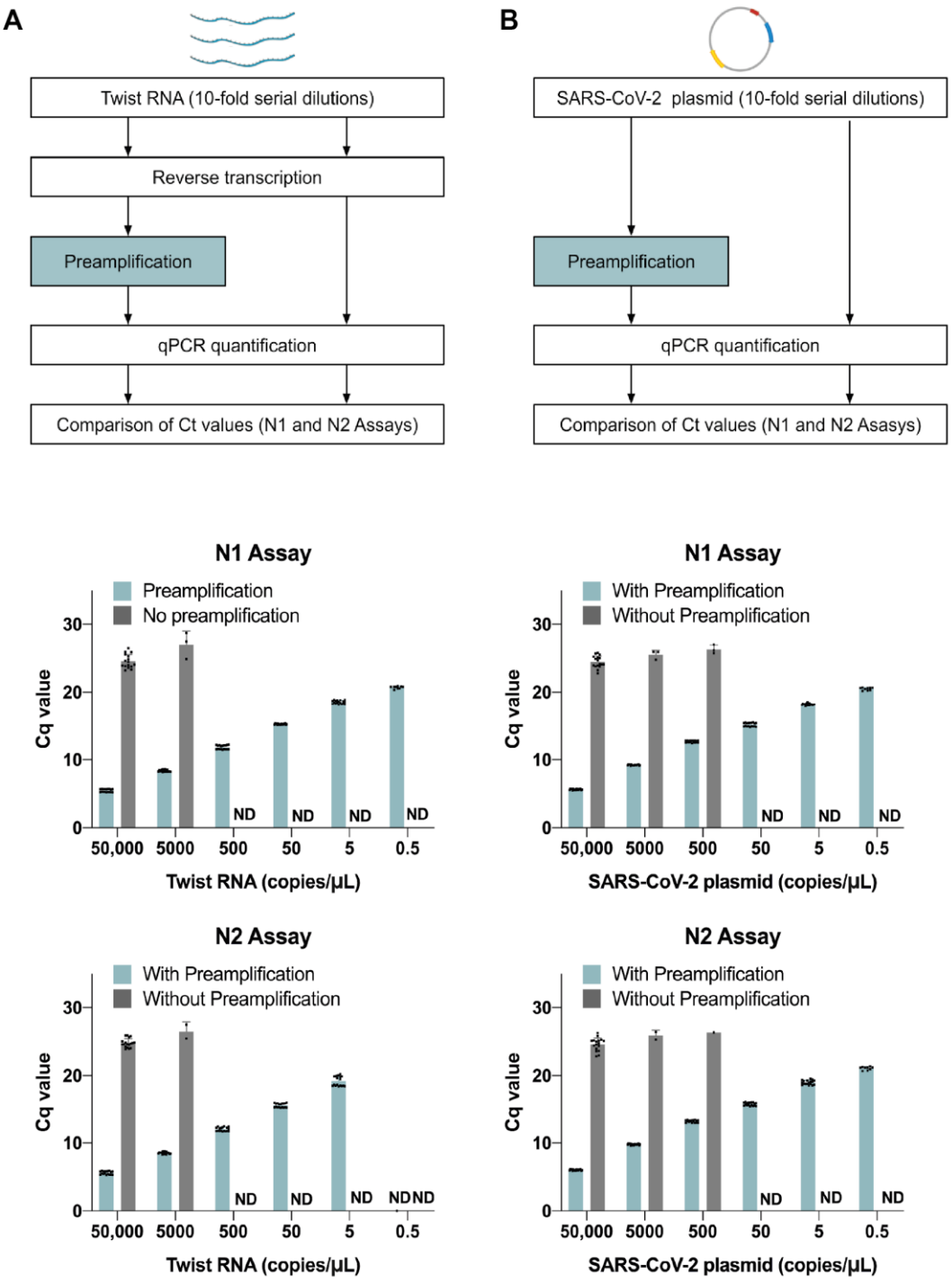

Figure 2. Preamplification leads to a lower limit of detection (LoD) in the microfluidic RT-qPCR method. Workflow for 10-fold serially diluted SARS-CoV-2 positive controls, with and without preamplification: (**A**) synthetic RNAs (Twist RNA) and (**B**) SARS-CoV-2 plasmid. Barplots show the Cq values with and without the preamplification step for both the N1 and N2 assays at each concentration. Data show the mean ± SD of valid Cq values from 18 replicates (2 biological replicates at each concentration, each with 9 technical replicates; each dot represents a technical replicate with a detected Cq value).

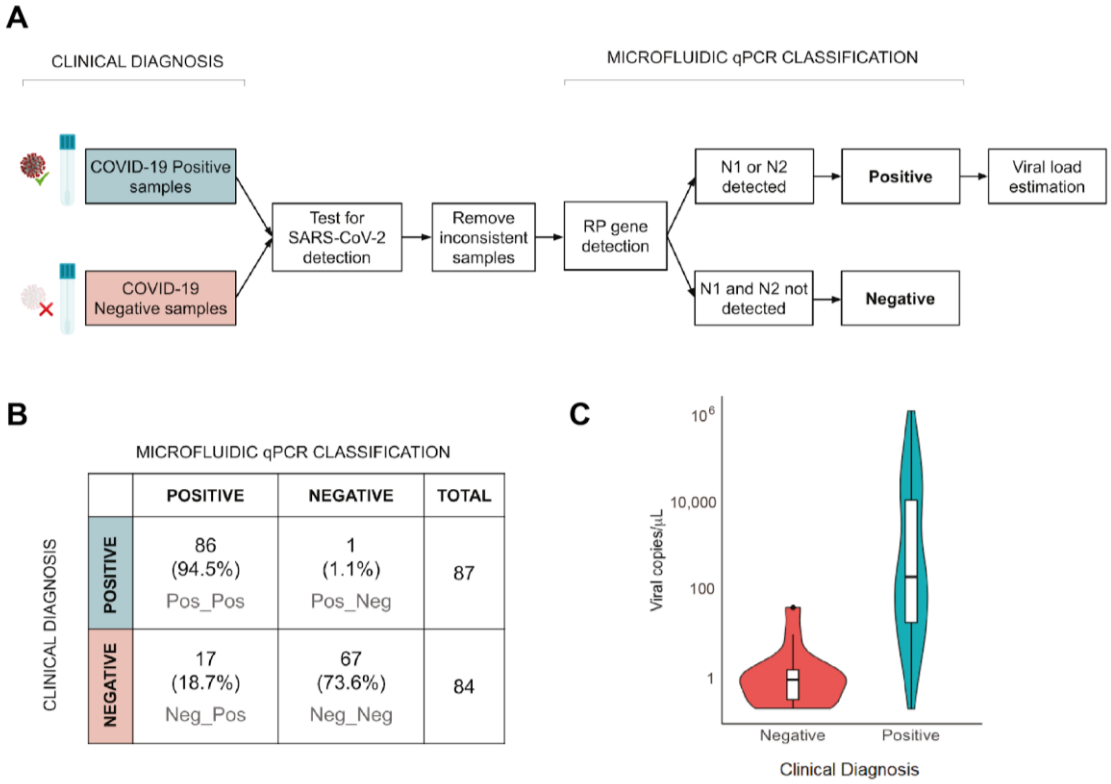

Figure 3. The three-step nano-scale RT-qPCR method shows higher sensitivity in detecting samples with low viral-loads. (**A**) Workflow for the re-analysis of clinical samples (SARS-CoV-2 positive and negative) from an accredited diagnostic lab. (**B**) Comparison between clinical diagnosis and the microfluidic qPCR classification. Category labels indicate clinical diagnosis followed by microfluidic qPCR classification (e.g., Neg_Pos = negative diagnosis, positive microfluidic qPCR result). (**C**) Viral load estimates for different categories of classified samples based on microfluidic qPCR. Samples with a negative clinical diagnosis contained very low viral loads (<100 copies/µL). Viral titers of samples in plate 1 and 2 were computed using the standard curve of plasmid controls from plate 1.

Standard curves are commonly used to estimate viral loads in RT-qPCR reactions, which is why we took that approach in our study. Standard curves based on 100-fold serial dilutions of Twist RNA and SARS-CoV-2 plasmids ranging from 5 to 50,000 copies/µL both showed a nearly-perfect log-linear fit ($R^2 > 0.99$) with little variation among technical replicates (SEM < 0.2) for both N assays (Figure S4). Having established technical precision using these curves, we used the SARS-CoV-2 plasmid standards to quantify viral copies in the clinical samples in each of the two PCR plates. Given that the N1 and N2 assays were highly concordant ($R^2 = 0.876$, Kendall's Tau correlation), and the difference in Cq values was within one cycle in over 90% of the samples (Figure S5A,B), we used an average Cq value for the N gene assays. To maximize consistency in viral load estimates among the samples, we then used the standard curve from plate 1 to quantify the viral loads in each clinical sample (Figure 3C). The Pos_Pos samples showed a wide range of estimated viral loads (0.2–1.17 × 10^6 viral copies/µL) spanning five orders of magnitude. In contrast, the Neg_Pos samples exhibited a much narrower range of viral load estimates (0.2–40.25 viral copies/µL), corresponding to very low amounts of viral material in the NP swab sample (0.05–10.73 viral copies/µL). These results show that the nano-scale qPCR method can detect SARS-CoV-2 across a broad range of viral titers and can confidently detect relatively low viral loads that could otherwise be missed by standard detection methods used in diagnostic labs.

To evaluate the reproducibility of this method in samples with low viral loads, we re-analyzed the 17 Neg_Pos samples after one and after two freeze cycles. After one freeze cycle, 11 samples remained positive, whereas after two freeze cycles, only 9 did (Figure 4A). This suggests that additional freeze cycles may lead to an increased false-negative rate, likely due to degradation of viral RNA resulting

in copy numbers below the LoD. This is consistent with prior observations of increased Cq values following one freeze–thaw cycle [27]. Nevertheless, 8 of the 17 samples were reproducibly classified as positive in three independent experiments (Figure 4B). When comparing viral load estimates among the 17 Neg_Pos samples, we found that the 11 samples that retested positive after one freeze cycle had viral loads between 0.21 and 38.89 copies/µL, whereas the 5 samples that retested negative all had viral loads less than 1 copy/µL based on the original experiment (Figure 4C). This suggests that samples with extremely low viral titers close to the LoD could fail to be consistently detected, likely due to factors such as sample degradation or stochastic variation in the number of viral RNA molecules present in the small reaction volumes used for RT.

A

	Original experiment	After one freeze cycle	After two freeze cycles
Positive	17	11	9
Negative	0	5	5
Inconsistent	0	1	3

B

After one freeze cycle \ After two freeze cycles	Positive	Negative	Inconsistent
Positive	8	2	1
Negative	1	2	2
Inconsistent	0	1	0

C

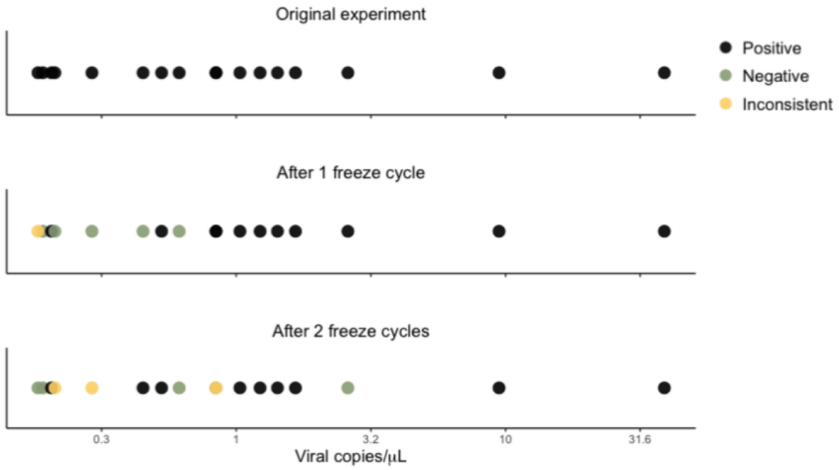

Figure 4. Reproducibility of results among the 17 Neg_Pos samples. (**A**) Summary of the microfluidic qPCR results across the original experiment and two replication experiments (after one freeze cycle and after two freeze cycles). (**B**) Cross-tabulation of microfluidic qPCR results in the two replication experiments. (**C**) Viral load estimates for the 17 Neg_Pos samples based on the original experiment. Color coding is based on the microfluidic qPCR results of the 17 samples in the two replication experiments, as either positive (black), negative (green), or inconsistent (yellow).

Lastly, we examined the relationship between the distributions of mean Cq values for the host RP gene assay and the N gene assay. If negative samples tended to show much higher Cq values for the RP assay than the positive samples, this would indicate that the negative result was likely due to inadequate sampling of human tissues in the swab. Instead, we observed no significant differences in the Cq values of RP assay between positive and negative samples (*t*-test, *p*-value = 0.08) (Figure 5A) and found minimal correlation between the mean Cq values of the RP and the N gene assays, with only 2.8% of the variation in the N gene assays attributable to detection of the RP gene (R^2 = 0.028, Kendall's Tau correlation) (Figure 5B). We thus conclude that the high Cq values for the N assays in the Neg_Pos samples were not due to inadequate sampling, but instead, accurately reflected low viral loads in these samples.

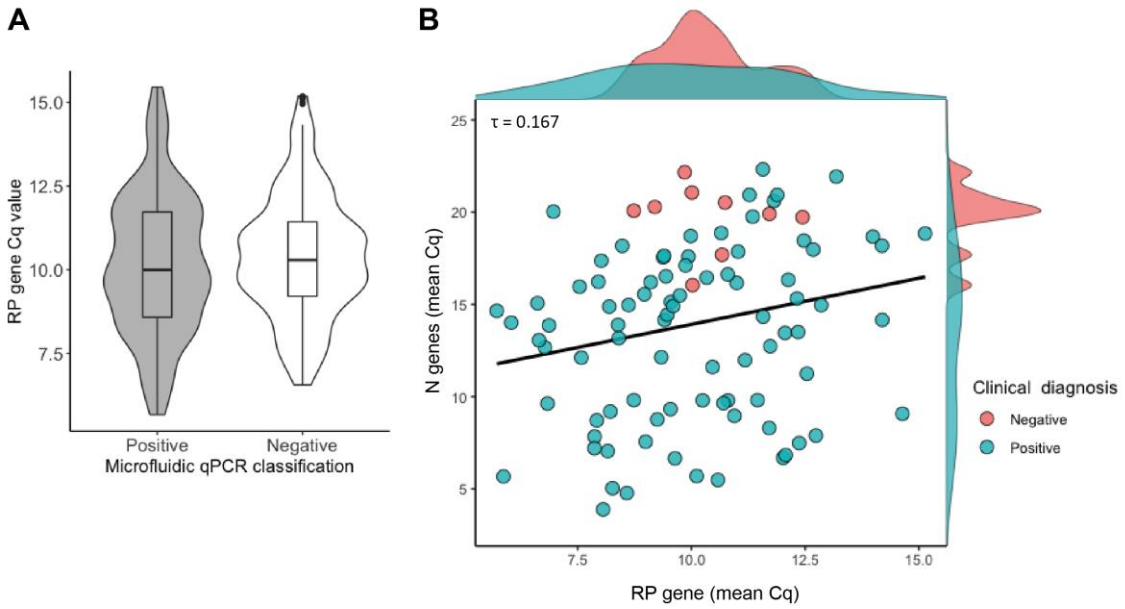

Figure 5. Low estimated viral titers are not due to poor quality samples. (**A**) Violin plots of RP gene Cq values across samples with positive and negative microfluidic qPCR results. There is no significant difference between the two groups (Welch's *t*-test, *p*-value = 0.08). (**B**) Scatter and density plots of N gene vs. RP gene Cq values from microfluidic qPCR for samples with negative or positive clinical diagnostic results. Cq values for viral N and host RP genes are not strongly correlated overall ($\tau = 0.167$, *p*-value = 0.017).

4. Discussion

In this study, we implement and validate a three-step approach for SARS-CoV-2 detection utilizing RT of SARS-CoV-2 viral RNA, cDNA preamplification, and nano-scale qPCR. Using serial dilutions of positive controls, we demonstrate a 1000-fold improvement in detection sensitivity of the microfluidic qPCR system when adding the preamplification step, consistent with a previous study in which a target preamplification step was found to enhance the LoD by 100-fold in detecting SARS-CoV [23]. We also show that nano-scale qPCR can be used to quantify viral copies in clinical samples with high confidence. Our data suggest that the LoD of this method (with preamplification) is less than 1 copy/µL: we obtained a LoD of 0.5 copies/µL for Twist RNA and SARS-CoV-2 plasmid, and detected the virus down to 0.2 copies/µL in experiments using clinical NP swab samples. Based on this analysis, our method seems to be more sensitive than standard RT-PCRs, which have reported a LoD ranging between 5.6 and 100 copies/µL [28–30], and that its performance is comparable to other highly sensitive methods such as the CDC 2019-nCoV RT-PCR Diagnostic Panel with QIAGEN QIAmp DSP Viral RNA Mini Kit and the QIAGEN EZ1 DSP (1 copy/µL) [3], ddPCR (0.1 copies/µL) [8], and RT-LAMP (1 copy/µL) [31].

Crucially, we demonstrate the power of this method to reduce the false-negative rate of SARS-CoV-2 clinical diagnostic tests: we detected SARS-CoV-2 in 17 samples diagnosed as negative by an accredited diagnostic lab with high confidence, based on a large number of technical replicates (9 for N1, 9 for N2, 6 for RP) and a conservative threshold for Cq value consistency among sample replicates (SEM < 0.5). This is especially important considering that the viral loads of these Neg_Pos samples (0.2–40.25 viral copies/µL) were close to the LoD of standard SARS-CoV-2 tests and are thus, more likely to return false-negative results using standard RT-PCR methods. This three-step microfluidics RT-qPCR method, which includes a preamplification step, nano-scale reactions, and a large number of replicates, can reliably detect samples with low viral load and reduce the false-negative rate compared to standard RT-PCR assays.

Beyond its ultra-sensitive detection of SARS-CoV-2, this microfluidic platform is a cost-effective strategy with several advantages: a nanoliter volume per reaction (lower reagent consumption per assay), a parallelized assay system (increased throughput), amenability to automation (increased precision), capacity to run a large number of replicates per sample (increased confidence in test results), and the capacity to simultaneously test for multiple pathogens (broader diagnostic utility). Based on our experience, and considering the fact that reagents cost more in the UAE than in Europe and the US, the cost of SARS-CoV-2 testing per sample using the 192.24 microfluidic chip and the design used in this study (9 replicates for N1 and N2, 6 replicates for RP) is approximately USD 17, including reagents and the chip, but excluding labor costs. This is approximately four times cheaper than the current cost of standard SARS-CoV-2 testing in the UAE. Lowering the number to three technical replicates for each of the N1, N2, and RP assays would allow for four additional assays, which can be utilized to diagnose other viral or bacterial infections using three technical replicates (or six additional assays with two technical replicates) at no extra cost, bringing down the cost per sample per assay even further. Since each sample is loaded only once and then analyzed against 24 assays simultaneously, no extra time is required for performing multiple assays of replicates. Because of this, the method has great potential for economies of scale, including assay multiplexing (to detect additional pathogens) and sample pooling (to increase throughput), which would further reduce per test costs. These advantages warrant serious consideration of this three-step nano-scale assay system, especially for active screening programs, which aim at the early detection of SARS-CoV-2 in asymptomatic, pre-asymptomatic, or mildly symptomatic individuals who likely carry low viral loads.

Supplementary Materials: The following are available online at http://www.mdpi.com/2227-9717/8/11/1425/s1, Figure S1: Fluidigm chip layout and N gene probes; Figure S2: Detection limit with RNA extraction step and the effect of carrier RNA; Figure S3: Consistency in Cq value ranking between the microfluidic RT-qPCR and the clinical diagnostic method; Figure S4: Linear regression of Cq values vs. copy number of serially diluted positive controls shows highly reproducible detection of SARS-CoV-2 across five orders of magnitude; Figure S5: Comparison of detection performance between N1 and N2 assays.

Author Contributions: Conceptualization, K.C.G., Y.I., and F.P.; methodology, X.X., Z.A., M.M.D., M.A., M.K., Y.M., F.A.J., and K.P.; software K.C.G., N.R., and C.A.J.; resources, L.E.M., Z.V., and M.Z.; formal analysis, T.G. and X.X.; writing—original draft preparation, X.X., T.G., K.C.G., Y.I., Z.A., and M.M.D., writing—review and editing, X.X., T.G., K.C.G., Y.I., Z.A., and M.M.D., funding acquisition, F.P., K.C.G., Y.I., and R.A. All authors have read and agreed to the published version of the manuscript.

Funding: This work was funded by support from NYU Abu Dhabi to the NYUAD Center for Genomics and Systems Biology (NYUAD Research Institute grant #ADHPG-CGSB1 to K.C.G.), NYUAD research grant AD105 (to Y.I.), the NYUAD Kawader Research Assistantship Program (to F.A.J.), and the NYUAD Core Technology Platforms.

Acknowledgments: This report is part of NYUAD's COVID Response Project. We thank members of NYU Abu Dhabi's (NYUAD) COVID-19 steering committee for spearheading and facilitating this project, including Ayaz Virji and Sehamuddin Galadari. We thank members of Proficiency Healthcare Diagnostics laboratory for sample collection and processing. We thank Michael Davis (Director of Laboratory Operations, NYUAD), Reza Rowshan (Director of Core Technology Platforms, NYUAD), Nizar Drou (Lead Developer, NYUAD Bioinformatics Core), Nada Messaikeh (Vice Provost for Research Administration, NYUAD), and Enas Qudeimat (Director of Operations, NYUAD-CGSB) for helping to make this work possible. We thank the Institutional Review Boards of the Abu Dhabi Department of Health and NYUAD and the NYUAD Institutional Biosafety Committee for expediting the review of this project and NYUAD Environmental Health and Safety for their support. This research was partially carried out using the Core Technology Platforms resources and the High-Throughput Screening (HTS) platform of CGSB at New York University Abu Dhabi.

Conflicts of Interest: The authors declare no conflict of interest. The funders had no role in the design of the study; in the collection, analyses, or interpretation of data; in the writing of the manuscript, or in the decision to publish the results.

References

1. World Health Organization (WHO). Laboratory Testing for 2019 Novel Coronavirus (2019-nCoV) in Suspected Human Cases, Interim Guidance, 2 March 2020. Available online: https://apps.who.int/iris/bitstream/handle/10665/331329/WHO-COVID-19-laboratory-2020.4-eng.pdf?sequence=1&isAllowed=y (accessed on 28 July 2020).
2. Corman, V.M.; Landt, O.; Kaiser, M.; Molenkamp, R.; Meijer, A.; Chu, D.K.; Bleicker, T.; Brünink, S.; Schneider, J.; Schmidt, M.L.; et al. Detection of 2019 novel coronavirus (2019-nCoV) by real-time RT-PCR. *Eurosurveillance* **2020**, *25*, 2000045. [CrossRef] [PubMed]
3. Centers for Disease Control and Prevention. Real-Time RT–PCR Panel for Detection 2019-nCoV (US Centers for Disease Control and Prevention, 2020). Available online: https://www.fda.gov/media/134922/download (accessed on 28 July 2020).
4. Dramé, M.; Teguo, M.T.; Proye, E.; Hequet, F.; Hentzien, M.; Kanagaratnam, L.; Godaert, L. Should RT-PCR be considered a gold standard in the diagnosis of COVID-19? *J. Med. Virol.* **2020**. [CrossRef]
5. Zhang, J.-F.; Yan, K.; Ye, H.-H.; Lin, J.; Zheng, J.-J.; Cai, T. SARS-CoV-2 turned positive in a discharged patient with COVID-19 arouses concern regarding the present standards for discharge. *Int. J. Infect. Dis.* **2020**, *97*, 212–214. [CrossRef] [PubMed]
6. Xiao, A.T.; Tong, Y.X.; Zhang, S. False negative of RT-PCR and prolonged nucleic acid conversion in COVID-19: Rather than recurrence. *J. Med. Virol.* **2020**, *92*, 1755–1756. [CrossRef]
7. Wikramaratna, P.; Paton, R.S.; Ghafari, M.; Lourenco, J. Estimating false-negative detection rate of SARS-CoV-2 by RT-PCR. *medRxiv* **2020**. [CrossRef]
8. Lu, R.; Wang, J.; Li, M.; Wang, Y.; Dong, J.; Cai, W. SARS-CoV-2 detection using digital PCR for COVID-19 diagnosis, treatment monitoring and criteria for discharge. *medRxiv* **2020**. [CrossRef]
9. Yu, F.; Yan, L.; Wang, N.; Yang, S.; Wang, L.; Tang, Y.; Gao, G.; Wang, S.; Ma, C.; Xie, R.; et al. Quantitative Detection and Viral Load Analysis of SARS-CoV-2 in Infected Patients. *Clin. Infect. Dis.* **2020**, *71*, 793–798. [CrossRef]
10. Guo, Y.; Wang, K.; Zhang, Y.; Zhang, W.; Wang, L.; Liao, P. Comparison and analysis of the detection performance of six new coronavirus nucleic acid detection reagents. *Chongqing Med.* **2020**, *14*, 1671–8348.
11. Kapitula, D.S.; Jiang, Z.; Jiang, J.; Zhu, J.; Chen, X.; Lin, C.Q. Performance & Quality Evaluation of Marketed COVID-19 RNA Detection Kits. *medRxiv* **2020**. [CrossRef]
12. Eisen, A.K.A.; Demoliner, M.; Gularte, J.S.; Hansen, A.W.; Schallenberger, K.; Mallmann, L.; Hermann, B.S.; Heldt, F.H.; De Almeida, P.R.; Fleck, J.D.; et al. Comparison Of Different Kits For SARS-CoV-2 RNA Extraction Marketed In Brazil. *bioRxiv* **2020**. [CrossRef]
13. Furukawa, N.W.; Brooks, J.T.; Sobel, J. Evidence Supporting Transmission of Severe Acute Respiratory Syndrome Coronavirus 2 While Presymptomatic or Asymptomatic. *Emerg. Infect. Dis.* **2020**, *26*. [CrossRef]
14. Gandhi, M.; Yokoe, D.S.; Havlir, D.V. Asymptomatic Transmission, the Achilles' Heel of Current Strategies to Control Covid-19. *N. Eng. J. Med.* **2020**, *382*, 2158–2160. [CrossRef] [PubMed]
15. Bai, Y.; Yao, L.; Wei, T.; Tian, F.; Jin, D.-Y.; Chen, L.; Wang, M. Presumed Asymptomatic Carrier Transmission of COVID-19. *JAMA* **2020**, *323*, 1406–1407. [CrossRef] [PubMed]
16. Rothe, C.; Schunk, M.; Sothmann, P.; Bretzel, G.; Froeschl, G.; Wallrauch, C.; Zimmer, T.; Thiel, V.; Janke, C.; Guggemos, W.; et al. Transmission of 2019-nCoV Infection from an Asymptomatic Contact in Germany. *N. Eng. J. Med.* **2020**, *382*, 970–971. [CrossRef]
17. Wang, C.; Liu, L.; Hao, X.; Guo, H.; Wang, Q.; Huang, J.; He, N.; Yu, H.; Lin, X.; Pan, A.; et al. Evolving epidemiology and impact of non-pharmaceutical interventions on the outbreak of Coronavirus disease 2019 in Wuhan, China. *medRxiv* **2020**. [CrossRef]
18. Ing, A.J.; Cocks, C.; Green, J.P. COVID-19: In the footsteps of Ernest Shackleton. *Thorax* **2020**, *75*, 693–694. [CrossRef] [PubMed]
19. Oran, D.P.; Topol, E.J. Prevalence of Asymptomatic SARS-CoV-2 Infection. *Ann. Intern. Med.* **2020**, *173*, 362–367. [CrossRef] [PubMed]
20. Li, R.; Pei, S.; Chen, B.; Song, Y.; Zhang, T.; Yang, W.; Shaman, J. Substantial undocumented infection facilitates the rapid dissemination of novel coronavirus (SARS-CoV-2). *Science* **2020**, *368*, 489–493. [CrossRef] [PubMed]

21. Zhou, R.; Li, F.; Chen, F.; Liu, H.; Zheng, J.; Lei, C.; Wu, X. Viral dynamics in asymptomatic patients with COVID-19. *Int. J. Infect. Dis.* **2020**, *96*, 288–290. [CrossRef]
22. Kucirka, L.M.; Lauer, S.A.; Laeyendecker, O.; Boon, D.; Lessler, J. Variation in False-Negative Rate of Reverse Transcriptase Polymerase Chain Reaction–Based SARS-CoV-2 Tests by Time Since Exposure. *Ann. Intern. Med.* **2020**, *173*, 262–267. [CrossRef]
23. Lau, L.T.; Fung, Y.-W.W.; Wong, F.P.-F.; Lin, S.S.-W.; Wang, C.R.; Li, H.L.; Dillon, N.; A Collins, R.; Tam, J.S.-L.; Chan, P.; et al. A real-time PCR for SARS-coronavirus incorporating target gene pre-amplification. *Biochem. Biophys. Res. Commun.* **2003**, *312*, 1290–1296. [CrossRef] [PubMed]
24. Parker, J.K.; Chang, T.-Y.; Meschke, J.S. Amplification of viral RNA from drinking water using TransPlex™ whole-transcriptome amplification. *J. Appl. Microbiol.* **2011**, *111*, 216–223. [CrossRef]
25. Jackson, J.B.; Choi, D.S.; Luketich, J.D.; Pennathur, A.; Ståhlberg, A.; Godfrey, T.E. Multiplex Preamplification of Serum DNA to Facilitate Reliable Detection of Extremely Rare Cancer Mutations in Circulating DNA by Digital PCR. *J. Mol. Diagn.* **2016**, *18*, 235–243. [CrossRef] [PubMed]
26. Del Gaudio, S.; Cirillo, A.; Di Bernardo, G.; Galderisi, U.; Thanassoulas, T.; Pitsios, T.; Cipollaro, M. Preamplification Procedure for the Analysis of Ancient DNA Samples. *Sci. World J.* **2013**, *2013*, 1–8. [CrossRef]
27. Li, L.; Li, X.; Guo, Z.; Wang, Z.; Zhang, K.; Li, C.; Wang, C.; Zhang, S. Influence of Storage Conditions on SARS-CoV-2 Nucleic Acid Detection in Throat Swabs. *J. Infect. Dis.* **2020**, *222*, 203–205. [CrossRef] [PubMed]
28. Han, M.S.; Seong, M.-W.; Kim, N.; Shin, S.; Cho, S.I.; Park, H.; Kim, T.S.; Park, S.S.; Choi, E.H. Viral RNA Load in Mildly Symptomatic and Asymptomatic Children with COVID-19, Seoul. *Emerg. Infect. Dis.* **2020**, *26*, 2497–2499. [CrossRef]
29. Wyllie, A.L.; Fournier, J.; Casanovas-Massana, A.; Campbell, M.; Tokuyama, M.; Vijayakumar, P.; Geng, B.; Muenker, M.C.; Moore, A.J.; Vogels, C.B.F.; et al. Saliva is more sensitive for SARS-CoV-2 detection in COVID-19 patients than nasopharyngeal swabs. *medRxiv* **2020**. [CrossRef]
30. Vogels, C.B.F.; Brito, A.F.; Wyllie, A.L.; Fauver, J.R.; Ott, I.M.; Kalinich, C.C.; Petrone, M.E.; Casanovas-Massana, A.; Muenker, M.C.; Moore, A.J.; et al. Analytical sensitivity and efficiency comparisons of SARS-COV-2 qRT-PCR assays. *medRxiv* **2020**. [CrossRef]
31. Yang, W.; Dang, X.; Wang, Q.; Xu, M.; Zhao, Q.; Zhou, Y.; Zhao, H.; Wang, L.; Xu, Y.; Wang, J.; et al. Rapid detection of SARS-CoV-2 using reverse transcription RT-LAMP method. *medRxiv* **2020**. [CrossRef]